Study of the Sintering Process Behavior on Some Structural and Physical Properties of (Ni-47Ti-3Cu) Alloy Prepared by Powder Metallurgy

Mustafa Khaled Nasef[1], Rasha Hamid Ahmed[1]

[1,2]*Tikrit University, Collage of Education for Pure Sciences ,Physics Department E-mail: mi230044pep@st.tu.edu.iq*

KEYWORDS
Alloys, Powder Metallurgy, Heat Treatment, Sintering, Physical Properties

ABSTRACT
This research aims to prepare the alloy (Ni-47Ti-3Cu) using powder metallurgy techniques and study the sintering behavior of this alloy at different temperatures. Powders of nickel, titanium, and copper, were mixed to ensure homogeneity, then compacted under a pressure of (5ton) for (2 min) to obtain cohesive samples. The sintering process was carried out at temperatures of (1050, 950, 850, 750, 650) °C for 1 hour. The structural properties were studied using X-ray diffraction (XRD), and the physical properties (apparent density, bulk density, porosity, and water absorption) were examined using Archimedes' principle-based tests. The XRD results indicated the emergence of a new phase with a different crystalline structure from the elements used in the preparation of the models, identified as (TiCuNi2) with a rhombohedral crystal system, while the constituent elements of the alloy exhibited face-centered cubic (F.C.C) structures for nickel and copper and a hexagonal close-packed (H.C.P) structure for titanium. The physical examination results showed that both apparent and bulk densities increased with increasing sintering temperature, while porosity and water absorption decreased with increasing sintering temperature.

1. Introduction

A mixture of elements with diverse properties can yield suitable characteristics for many engineering applications, often surpassing those of pure elements [1]. An alloy, which is a mixture formed from the complete or partial union of two or more chemical elements, typically exhibits superior properties compared to the base metal involved [2]. The (Ni-50Ti-4Cu) alloy is an attractive choice for applications requiring a combination of exceptional structural and physical properties, such as machine parts and equipment operating in harsh environments, due to its structural stability, durability, high corrosion resistance, excellent formability, and high-temperature resistance [3-5]. Nickel is known for its good mechanical properties and high corrosion resistance. It also easily combines with many metals, making it a component of many important alloys, including (Ni-Ti) [6]. Titanium exhibits properties similar to steel, with high mechanical resistance and significant corrosion resistance, but it is lighter than steel [7,8]. It is used in many alloys alongside iron, aluminum, nickel, and other elements to produce strong and lightweight alloys [9]. Copper is notable for its ease of forming, high electrical conductivity, and wide range of alloys, including brasses, bronzes, and cupronickels, where copper is added to nickel to enhance mechanical properties and reduce alloy costs [10]. There are several methods for preparing alloys, one of which is powder metallurgy. This technique is valuable for creating a variety of microstructures and producing materials with all the distinctive physical, chemical, and mechanical properties, allowing the manufacture of products from almost any metal, including alloys that cannot be produced using traditional metallurgical methods [11,12]. Sintering is one of the most crucial thermal treatments for cold-pressed products. It involves heating the product to (70-90) % of the metal's melting temperature to reduce porosity and achieve a dense and hard structure. Cold-pressed products have low green strength, necessitating the enhancement of their mechanical and physical properties through the irreversible process of sintering [13,14].

2. Experimental part

The (Ni-50Ti-4Cu) alloy was prepared using powder metallurgy techniques. The first step in sample preparation involved procuring the powders of the elements used in this study: nickel (Ni) and copper with 99.95% purity from Buchs Fluka AG (Germany), and titanium powder with 99.99% purity from Sky Spring Nanomaterials (USA). These powders were weighed using a precise balance (Sartorius) of Japanese origin with an accuracy of 0.0001 according to the following ratios: (46% Ni + 50% Ti + 4% Cu). The powders were then mixed manually for half an hour using an agate mortar to achieve homogeneity. After mixing, a homogeneous powder mixture was obtained. The compaction process

was conducted using uniaxial pressing. The mixture was placed in a high-density steel mold with excellent mechanical properties, which was then inserted into a uniaxial hydraulic press (HONMAKSAN) of Turkish origin and compressed under a pressure of (5ton) for (2 min) to avoid elastic rebound. Six samples of the alloy were produced. The sintering process followed, using a CARBOLITE electric furnace (German origin) at temperatures of °C (1050, 950, 850, 750, 650) for 1 hour. To determine the structural properties, the samples were examined using X-ray diffraction (XRD) with a PANALYTICAL'S AERIS device of American origin, and International Centre for Diffraction Data (ICDD) cards were used. The physical properties (apparent density, bulk density, apparent porosity, and water absorption) were measured using Archimedes' principle-based physical tests.

3. Results and Discussion

Structural Properties

X-ray Diffraction (XRD) Analysis

This technique was employed to understand the crystalline structure of the prepared alloy and to observe the effect of increased sintering temperature on this structure. Before sintering, XRD analysis, aided by ICDD cards, showed only the peaks of the basic materials, indicating that the main components of the alloy (Ti, Ni, Cu) were in an unreacted state and no new compounds had formed. According to Table (1), nickel appeared at angles (°44.2583 , 76.9792°) with Miller indices (111), (220), according to card number (03-065-2865), and copper appeared at angles (°43.0907, °72.3016)with Miller indices (111), (220), according to card number (01-085-1326). Thus, the crystalline structure of both nickel and copper was face-centered cubic (F.C.C). Titanium appeared at angles (°35.8834, °39.1697, °40.936, °52.5847, °77.0167) with Miller indices (100), (002), (101), (102), (201), according to card number (00-001-1197), indicating a hexagonal crystal structure for titanium. After sintering, a new phase (TiCuNi2) was observed in all samples. This new ternary alloy with a rhombohedral crystal system appeared at angles (°28.9164 , °54.7647 ,°63.2788) ،with Miller indices (002), (200), (114), according to card number (00-101-0026). This indicates an atomic exchange reaction among the alloying elements and the formation of new bonds, resulting in the (TiCuNi2) phase during sintering, significantly impacting the structural, physical, and mechanical properties [15]. Moreover, with increasing sintering temperature, the intensity peaks of the primary materials (which remained after sintering) decreased, as illustrated in Figures (1), (2), (3), (4), (5), and (6). This was due to the reaction during sintering, leading to the transformation of some primary materials into the (TiCuNi2) compound with a different structure and changes in crystalline properties due to the high temperatures. Additionally, the intensity peaks of the (TiCuNi2) compound increased with higher temperatures, especially in sample (5) at 950°C, then slightly decreased in sample (6) at 1050°C. The reason is that the temperature ranges from 650°C to 950°C promoted the formation and homogeneity of this compound's crystalline structure, while the slight decrease in intensity at 1050°C could be attributed to changes in the crystalline properties (irregular crystalline surfaces) and increased grain growth [16].

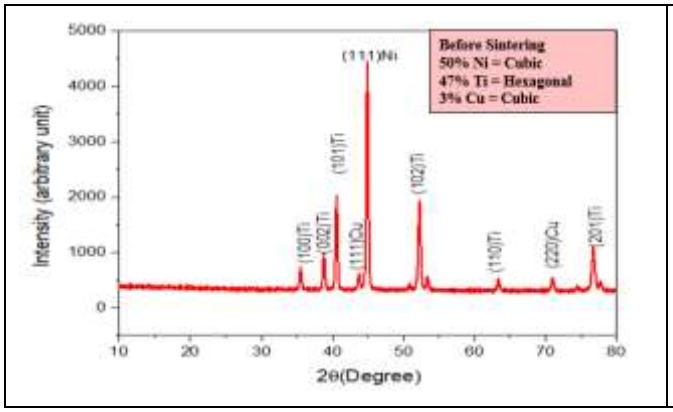

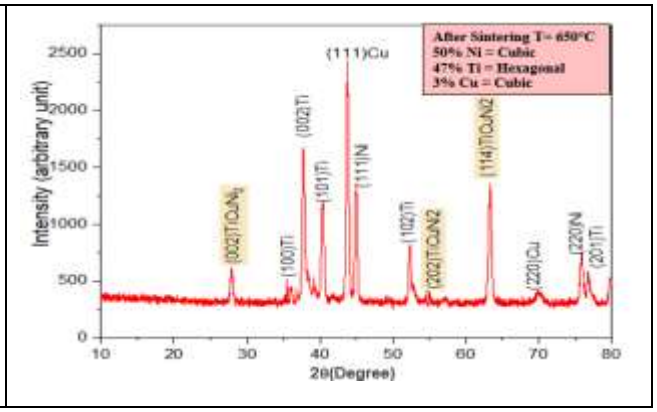

Fig. (1) X-ray diffraction of sample (1) before sintering

Fig. (2) X-ray diffraction of sample (2) at a temperature of (650°C)

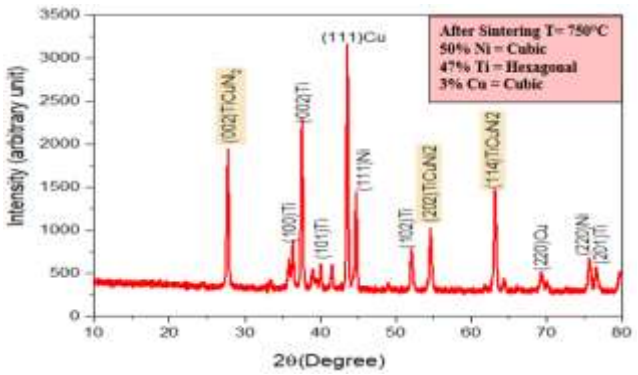

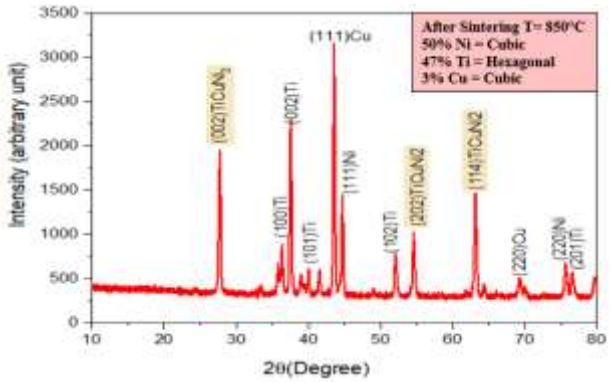

Fig. (3) X-ray diffraction of sample (3) at a temperature of (750°C)

Fig. (4) X-ray diffraction of sample (4) at a temperature of (850°C)

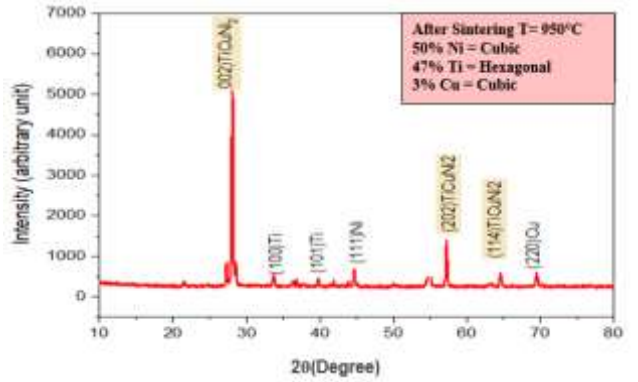

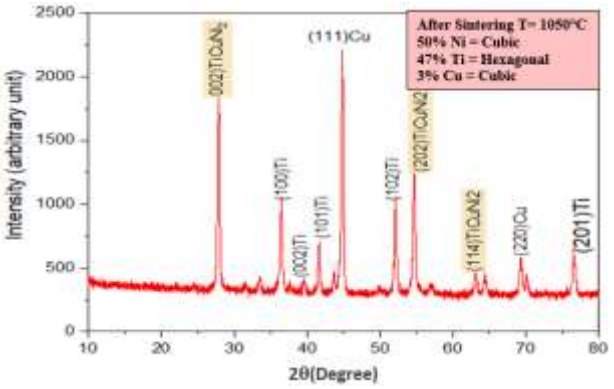

Fig. (5) X-ray diffraction of sample (5) at a temperature of (950°C)

Fig. (6) X-ray diffraction of sample (6) at a temperature of (1050°C)

Table (1) X-ray diffraction results before and after sintering

Temperatures (°C)	**2Theta (Degree)**	**FWHM (Deg)**	**d_{hkl} Exp (°A)**	**C.S (nm)**	**hkl**	**Phase**	**System**	**Card No**
Before Sintering	35.8834	0.1864	2.50057	53.16678975	(100)	Ti	Hexagonal	**00-001-1197**
	39.1697	0.1863	2.29801	55.59222847	(002)	Ti	Hexagonal	**00-001-1197**
	40.936	0.1945	2.20284	54.64671388	(101)	Ti	Hexagonal	**00-001-1197**
	43.0907	0.1763	2.05227	62.36588454	(111)	Cu	Cubic	**01-085-1326**
	44.2583	0.1918	2.002	58.4522602	(111)	Ni	Cubic	**03-065-**

				4				**2865**
	52.5847	0.2433	1.78239	54.31671306	(102)	Ti	Hexagonal	**00-001-1197**
	72.3016	0.2591	1.73901	101.937628	(220)	Cu	Cubic	**01-085-1326**
	76.9792	0.3847	1.70471	92.63864309	(220)	Ni	Cubic	**03-065-2865**
	77.0167	0.2531	1.46057	141.2060248	(201)	Ti	Hexagonal	**00-001-1197**
650	28.9164	0.4219	3.19342	21.53792964	(002)	TiCuNi2	rhombohedral	**00-101-0026**
	35.4111	0.2806	2.53284	35.11002843	(100)	Ti	Hexagonal	**00-001-1197**
	38.5352	0.5735	2.33438	17.89861055	(002)	Ti	Hexagonal	**00-001-1197**
	40.3886	0.1829	2.23142	57.63758283	(101)	Ti	Hexagonal	**00-001-1197**
	43.7542	0.3375	2.06727	32.93710127	(111)	Cu	Tetragonal	**01-085-1326**
	44.9561	0.2966	2.01475	38.255694	(111)	Ni	Cubic	**03-065-2865**
	52.3238	0.2849	1.74707	46.1115948	(102)	Ti	Hexagonal	**00-001-1292**
	54.7647	0.3562	1.67483	39.07180315	(200)	TiCuNi2	rhombohedral	**00-101-0026**
	63.2788	0.4179	1.46844	42.73052576	(114)	TiCuNi2	rhombohedral	**00-101-0026**
	70.163	1.17	1.34025	20.22352523	(220)	Cu	Cubic	**01-085-1326**
	75.8052	0.4302	1.2539	76.11311788	(220)	Ni	Cubic	**03-065-2865**
	76.7675	0.4219	1.24057	90.68733649	(201)	Ti	Hexagonal	**00-001-1197**
750	28.0683	0.1983	2.23226	45.47838455	(002)	TiCuNi2	rhombohedral	**00-101-0026**
	35.4955	0.1703	2.06107	57.91082293	(100)	Ti	Hexagonal	**00-001-1197**
	39.3382	0.2857	2.01074	36.33794546	(002)	Ti	Hexagonal	**00-001-1197**
	40.3729	0.1628	1.74446	64.73868192	(101)	Ti	Hexagonal	**00-001-1197**
	43.8927	0.1749	1.67057	63.70549611	(111)	Cu	Tetragonal	**01-085-1326**
	44.0507	0.1727	1.46537	65.81002343	(111)	Ni	Cubic	**03-065-2865**
	52.4079	0.1907	1.3493	69.0205868	(102)	Ti	Hexagonal	**00-001-1292**
	54.9161	0.2187	1.25255	63.87601915	(200)	TiCuNi2	rhombohedral	**00-101-0026**
	63.4265	0.2535	1.23926	70.8049671	(114)	TiCuNi	rhombohedr	**00-101-**

				7		2	al	**0026**
	69.6244	0.5021	2.23226	45.93033401	(220)	Cu	Cubic	**01-085-1326**
	75.9017	0.3418	2.06107	96.44060905	(220)	Ni	Cubic	**03-065-2865**
	76.8632	0.1889	2.01074	87.0241243	(201)	Ti	Hexagonal	**00-001-1197**
850	28.3296	0.1013	3.26065	89.2229227	(002)	TiCuNi2	rhombohedral	**00-101-0026**
	35.7268	0.2144	2.44506	46.72599899	(100)	Ti	Hexagonal	**00-001-1197**
	37.8762	0.2433	2.37346	41.80988514	(002)	Ti	Hexagonal	**00-001-1197**
	39.8107	0.2078	2.26247	50.30200192	(101)	Ti	Hexagonal	**00-001-1197**
	43.9024	0.2303	2.06063	48.3886518	(111)	Cu	Tetragonal	**01-085-1326**
	44.7005	0.2439	2.02568	46.31584566	(111)	Ni	Cubic	**03-065-2865**
	52.3799	0.2698	2.00993	48.75418054	(102)	Ti	Hexagonal	**00-001-1292**
	54.9291	0.2138	1.74533	65.36108426	(200)	TiCuNi2	Rhombohedral	**00-101-0026**
	63.3507	0.3231	1.67021	55.40614607	(114)	TiCuNi2	Rhombohedral	**00-101-0026**
	70.3216	0.2909	1.46694	81.96829829	(220)	Cu	Cubic	**01-085-1326**
	75.98	0.2354	1.33762	140.7976927	(220)	Ni	Cubic	**03-065-2865**
	76.7919	0.3053	1.24023	115.1048403	(201)	Ti	Hexagonal	**00-001-1197**
950	28.5275	0.1561	3.12639	58.5459125	(002)	TiCuNi2	rhombohedral	**00-101-0026**
	35.6361	0.2485	2.4509	40.26659318	(100)	Ti	Hexagonal	**00-001-1197**
	44.621	0.1626	2.0291	69.37857118	(111)	Ni	Cubic	**03-065-2865**
	54.8489	0.1693	1.67246	82.37688798	(200)	TiCuNi2	rhombohedral	**00-101-0026**
	57.1949	0.1495	1.60931	99.13297883	(202)	TiCuNi2	rhombohedral	**00-101-0026**
	63.1681	0.498	1.47074	35.72057596	(114)	TiCuNi2	rhombohedral	**00-101-0026**
	70.2464	0.1897	1.33887	125.2367364	(220)	Cu	Cubic	**01-085-1326**
1050	28.3353	0.1699	3.14716	53.69296095	(002)	TiCuNi2	rhombohedral	**00-101-0026**
	35.9389	0.2227	2.43151	44.53185409	(100)	Ti	Hexagonal	**00-001-1197**
	40.0413	0.1592	2.24997	65.8795443	(101)	Ti	Hexagonal	**00-001-**

				7				**1197**
	44.8972	0.157	2.01726	72.19751953	(111)	Ni	Cubic	**03-065-2865**
	54.136	0.1425	1.66443	98.57221845	(200)	TiCuNi2	rhombohedral	**00-101-0026**
	57.4548	0.1269	1.60264	117.6167777	(202)	TiCuNi2	rhombohedral	**00-101-0026**
	63.4646	0.5165	1.46458	34.79759402	(114)	TiCuNi2	rhombohedral	**00-101-0026**
	70.5442	0.1254	1.33394	192.237987	(220)	Cu	Cubic	**01-085-1326**

Secondly: Physical Properties

The results for apparent density, bulk density, apparent porosity, and water absorption of the alloy samples were obtained through physical tests based on Archimedes' principle.

Apparent Density

Figure (7) illustrates the relationship between the apparent density ratios as a function of varying sintering temperatures ºC (650, 750, 850, 950, 1050) for the alloy samples. Table (2) presents the apparent density ratios for these samples, where the following observations were made The apparent density of the alloy samples increased after sintering compared to before sintering. This increase is due to the thermal expansion of the grains, which leads to the reduction of porosity, thereby increasing the apparent density [17, 18, 19]. The apparent density increases with rising sintering temperature. This can be attributed to the fact that higher temperatures enhance the bonding strength between the particles of the sample's constituent elements, thereby reducing porosity and increasing apparent density [20]. The crystal structure and grain size change to a more interconnected and dense structure, as indicated by the formation of the (TiCuNi2) compound according to XRD results [21]. The apparent density begins to decrease at the sintering temperature of 1050°C, being lower than at 950°C. This can be explained by the fact that sintering at such a high temperature leads to changes in the shape and distribution of the pores, increasing their diameter. Most of the smaller pore's merge into larger ones, which negatively affects the overall density, including the apparent density [22].

Table (2) Apparent Density ratios of alloy samples

Temperature (C°)	Apparent Density (g/cm^3)
Before Sintering	1.31
650	1.60
750	1.81
850	1.97
950	2.31
1050	2.01

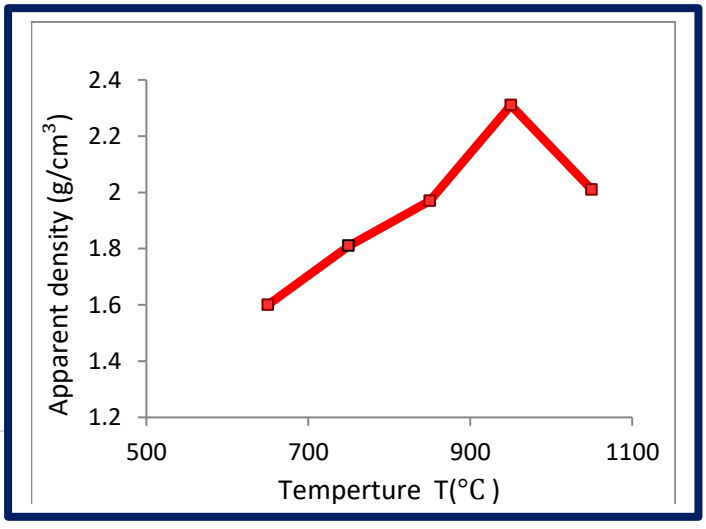

Fig. (7) The relationship between Apparent Density ratios as a function of changing sintering

Bulk Density

Figure (8) shows the relationship between bulk density ratios as a function of varying sintering temperatures (650, 750, 850, 950, 1050) ºC for the alloy samples. Table (3) presents the bulk density ratios for these samples, determined based on Archimedes' principle, both before and after sintering. The following observations were made: The bulk density of the alloy samples increased after sintering compared to before sintering. This increase is due to solid-state diffusion, which leads to an increase in bulk density [23]. The bulk density increases with rising sintering temperature. This can be attributed to the fact that higher temperatures lead (in addition to solid-state diffusion) to the fusion of the particles of the constituent elements of the sample. The similar densities of nickel and copper (8.90 g/cm³ for nickel and 8.95 g/cm³ for copper) facilitate this fusion [23]. This fusion results in a rearrangement of atoms or molecules in the crystal lattice, changing the crystal structure and forming new phases, as indicated by XRD analysis (formation of the TiCuNi2 phase). Occasionally, lattice compression may also occur. All these factors undoubtedly lead to an increase in bulk density [24].

The bulk density begins to decrease at the sintering temperature of 1050°C, being lower than at 950°C. This can be explained by the fact that sintering at such a high temperature leads to increased diffusion of nickel and copper into titanium. Elements with lower melting points (nickel and copper) will diffuse into the element with a higher melting point (titanium in this case). As a result, regions in the sample that are rich in nickel and copper will experience material loss due to the migration of atoms, leading to an imbalance in void distribution across the regions. These regions will eventually reach supersaturation, resulting in the formation of pores due to the accumulation of voids, and consequently, a slight decrease in bulk density [25].

Table (3) Bulk Density ratios of alloy

Temperature (C°)	Bulk Density (g/cm^3)
Before Sintering	1.23
650	1.37
750	1.49
850	1.54
950	1.91
1050	1.76

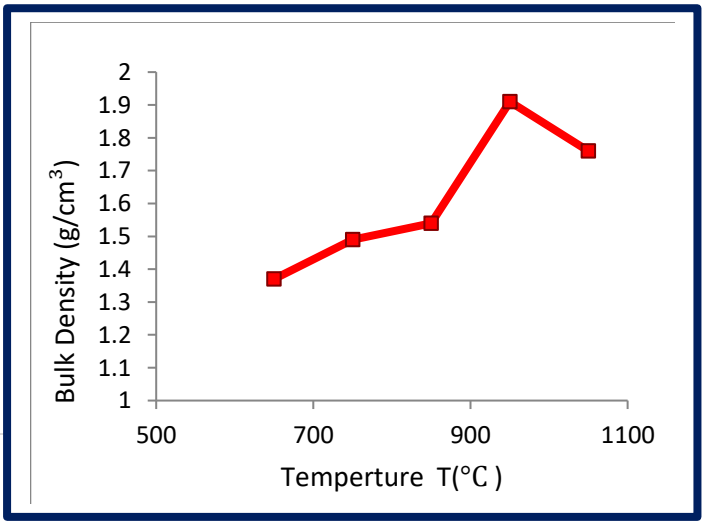

Fig. (8) The relationship between Bulk Density ratios as a function of changing sintering

Porosity and Water Absorption

Figure (9) illustrates the relationship between apparent porosity ratios as a function of varying sinterng temperatures (650, 750, 850, 950, 1050ºC). Figure (10) shows the relationship between water absorption ratios as a function of the same sintering temperature range. Table (4) presents the apparent porosity ratios for the alloy samples, while Table (5) presents the water absorption ratios for these samples. The following observations were made: Upon sintering the samples, both apparent porosity and water absorption decreased compared to their values before sintering. This decrease is attributed to the role of heat in enhancing the bonding between the particles of the sample elements, which reduces overall porosity, particularly apparent porosity. Since absorption depends on porosity where water absorption requires the presence of voids (open pores) between the material particlesreducing apparent porosity will also reduce water absorption [26]. With an increase in sintering temperature, apparent porosity and water absorption continue to decrease. This is because higher sintering temperatures lead to stronger bonds between the particles of the sample elements as atoms and molecules occupy more optimal positions due to the heat, promoting grain growth. Consequently, the shape and size of the pores change and diminish consistently [24]. Additionally, the formation of more compact phases, such as the TiCuNi2 phase identified by XRD analysis, contributes to the elimination of many pores, thereby reducing water absorption as well [27].

At a sintering temperature of 1050°C, both apparent porosity and water absorption start to rise slightly, becoming marginally higher than at 950°C. This can be explained by the increased diffusion of nickel and copper into titanium at this high temperature. Regions in the sample that are rich in nickel and copper will experience material loss as they lose more atoms, disrupting the balance of voids in one area compared to another. The aggregation of these voids leads to pore formation, resulting in a slight increase in apparent porosity and consequently, water absorption as well at the temperature of 1050°C [25].

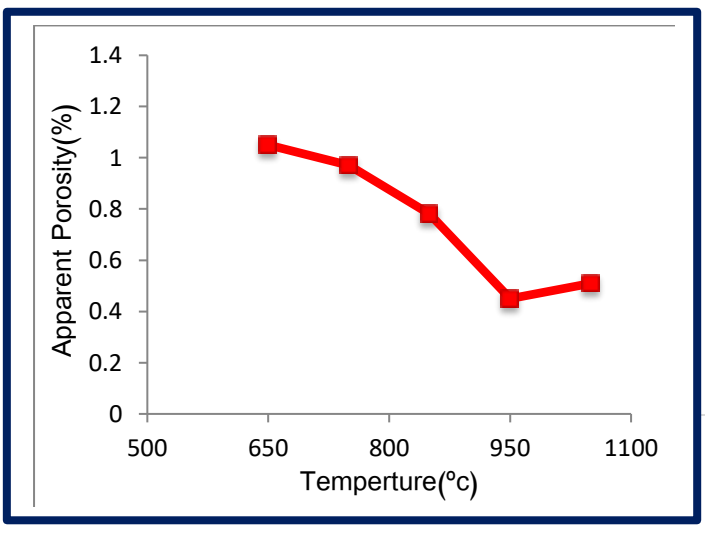

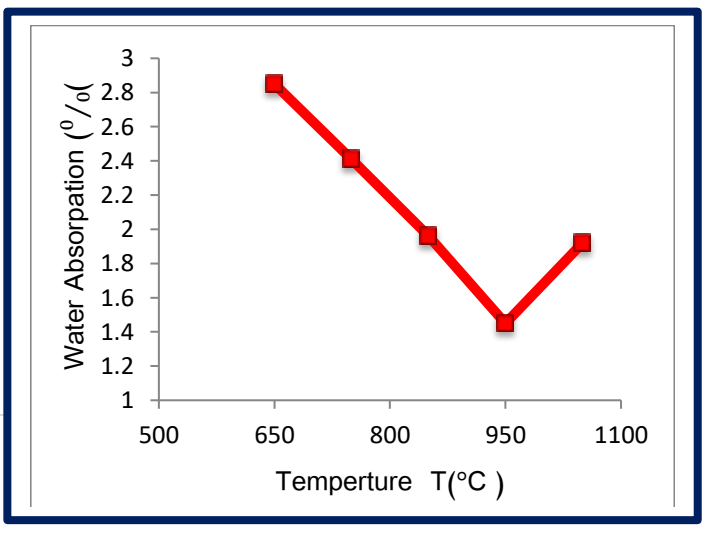

Figure (9) Relationship between apparent porosity as a function of changing sintering temperature

Fig. (10): The relationship between water absorbency as a function of changing sintering. temperature

Table (4) Apparent porosity ratios of alloy samples

Temperature (°C)	Apparent porosity (%)
Before Sintering	1.01
650	1.05
750	0.97
850	0.78
950	0.45
1050	0.51

Table (5) Water absorption percentage of alloy

Temperature (°C)	Water Absorption (%)
Before Sintering	3.04
650	2.85
750	2.41
850	1.96
950	1.45
1050	1.92

4. Conclusions:

After conducting tests on the study samples, the following conclusions were reached: The preparation method used (powder metallurgy technique) was successful. It is possible to obtain a new phase different from the phases of the original alloy components. The phase (TiCuNi2) with a rhombohedral crystal system was obtained, while the crystal systems of the elements forming the alloy are face-centered cubic (F.C.C) and hexagonal. A sintering time of one hour helped improve the properties of the studied alloy depending on the temperatures. The best apparent and bulk density values for the alloy were at a temperature of 950°C, where they reached their highest value. The best porosity and water absorption rates for the alloy were at a temperature of 950°C, where they reached their lowest value. From all the above, it is clear that the best sintering temperature for the studied alloy is 950°C for one hour.

Reference

[1] William D. Callister, Jr., David G. Rethwisch " Fundamentals of Materials Science and Engineering: An Integrated Approach", John Wiley & Sons Publications, 4th Edition, (2012), pp.4.

[2] Adel Mahmoud Hassan and Fidaa Safaa Muhammad Ali, “Principles of Mineralogy,” Part One, University of Mosul, Directorate of Dar Al-Kutub for Printing and Publishing, 1986.

[3] Mohammed Rahman, Ayad M. Takhakh “An investigation to the Effect of Copper Addition on the Characteristics of Ni-Ti Shape Memory Alloy", Al-Nahrain Journal Engineering Sciences, Vol.19, No.1, (2016) PP.86-91.

[4] Dania F. Abbas Aljuboori, Kadhim K. Resan, Ayad M. Takhakh “Investigate the Microstructure and the Mechanical Properties of Ni-Ti-Cu Shape Memory Alloys", Al-Nahrain Journal, Engineering Sciences, Vol.20, No.1, (2016) PP.105-112,

[5] Oshida, Yoshiki and Tominaga, Toshihiko. Nickel-Titanium Materials: Biomedical Applications, Berlin, Boston: De Gruyter, (2020), PP.25-31, 210-212, https://doi.org/10.1515/9783110666113

[6] Issa Masoud Baghni, “Fundamentals of Materials Engineering”, Libyan Republic, Libyan Authority for Research, Science and Technology, Media and Publishing Department, National Library - Benghazi, First Edition, 2014, p. 145.

[7] Aidh bin Saad Marzan Al-Shahri, Muhammad Ali Khalafah Saleh, Dr. Hussein Muhammad Abdul Fattah Ali, “Chemistry of Transitional Elements”, Al-Obeikan Publishing Foundation, First Edition, 2005, p. 255.

[8] Matthew J. Donachie, "Titanium a technical Guide", second Edition, pp 2-4, 2000.

[9] Hassan Bouzian, “A detailed analytical chemical study of the elements of the periodic table,” Part One, Algeria (n.d.), 2017, pp. 143-146.

[10] Qahtaan Khalaf Al-Khazraji, “Non-ferrous metals and their alloys,” Dijlah Publishing House, First Edition, 2009, Republic of Iraq, p. 20

[11] A. K. Sinha " Powder Metallurgy " Ianpat Rai Publications (P) LTD., Daryaganj, New Delhi, (1987). P.P22

[12]G. Dowson "Powder Metallurgy: The Process and Its Products", Springer Netherlands, (1990), P.P11.

[13] Barmakov Vyaznikov “The use of powder metallurgy in industry”, Moscow, Mir Publishing House, first edition, 1968.

[14] G. S. Upadhyaya " Powder Metallurgy Technology " Published by Cambridge International Science Publishing, England, 2002.

[15] Y. Zhang, J. L. Jin and Z. O. Ji, "Two-stage Transformation and Reverse Process in a Ti-Ni-Cu Alloy" International Journal of Materials Research, vol. 86, no. 2, pp. 91-96, 1995.

[16] Song K., Aindow M. Grain growth and particle pinning in a model Ni-based superalloy. Mater. Sci. Eng. A. 2008; 479:365–372. doi: 10.1016/j.msea.2007.09.055.

[17] A. Varea, Eva Pellicer, Salvador Pané, Bradley J. Nelson, Santiago Suriñach, Maria Dolors Baró and Jordi Sort " Mechanical Properties and Corrosion Behaviour of Nanostructured Cu-rich Cu Ni Electrodeposited Films" Int. Journal. Electrochemical. Science, vol 7, p.p(1288 – 1302), 2012.

[18] H.J.Chang, J.S.Rho, and Y.C. Chang ‘‘Optical and Electrical Properties of Thin Film Electroluminescent Devices With SrS : Cu , Ag Phosphor Layer’’ Journal of the Microelectronics & Packaging Society Vol. 9, No.1, PP 29-33, 2002.

[19] R. Monzen, Y Shimada and C Watanabe "Mechanical properties of Cu-Ni-Be system alloys" Journal of Physics, 15th International Conference on the Strength of Materials (ICSMA-15), 2010.

[20] A.V area, Eva Pellicer, Salavador Pane, Btadley J. Nelson, Santiayo, Surinach Maria Dolors Baro and Jordi Sort "Mechanical Properties and corrosion Behaviour of Nanstruetred CU- rich CU Ni Electrodeposited Film" In. Journal – Electrochemical. Science, Vo17, (2012), p.p (1288-1302).

[21] Woodward, C., and S. Kajihara. "Density of thermal vacancies in γ-Ti–Al–M, M= Si, Cr, Nb, Mo, Ta or W." Acta materialia 47.14 (1999): 3793-3798.

[22] Tomasz, Goryczka,"Ni25Ti50Cu25 shape memory alloy produced by nonconventional techniques" Shape Memory Alloys: Processing, Characterization and Applications, Dr. Francisco Manuel Braz Fernandes, pp.53-76, 2013.

[23] Celebi Efe, T. Yener, I. Altinsoy, M. Ipek, S. Zeytin, C. Bindal, " Characterization of Cemented Cu Matrix Composites Reinforced with SiC ", Sakarya University, Engineering Faculty, Department of Metallurgy and Materials Engineering, Esentepe Campus, 54187 Sakarya, Turkey, Vacuum 85 pp 643-647 (2010).

[24] Henriques, V. A. R., et al. "Microstructural evolution during hot pressing of the blended elemental Ti–6% Al–7% Nb alloy." Materials Science and Engineering: A 347.1-2 (2003): 315-324.

[25] Rasha Hamid Ahmed, “Study of the structural and mechanical properties of the copper-nickel binary system alloy prepared using powder technology,” Master’s thesis, Tikrit University, College of Education for Pure Sciences, Department of Physics, 2013, pp. 53-59.

[26] Aqeel Ali Nazim, Mahdi Matar Hanoun, “The effect of adding silicon carbide powder on the properties of nickel-copper, produced using powder technology,” Journal of Engineering and Technology, Volume 29, Issue 11, 2011, p. 497.

[27] Yılmaz, Eren, et al. "Mechanical properties and electrochemical behavior of porous Ti-Nb biomaterials." Journal of the mechanical behavior of biomedical materials 87 (2018): 59-67.